

Damage detection in multilayered fiber–metal laminates using guided-wave phased array[†]

Ameneh Maghsoodi^{1,*}, Abdolreza Ohadi¹, Mojtaba Sadighi¹ and Hamidreza Amindavar²

¹Department of Mechanical Engineering, Amirkabir University of Technology, Tehran, Iran

²Department of Electrical Engineering, Amirkabir University of Technology, Tehran, Iran

(Manuscript Received August 9, 2015; Revised January 5, 2016; Accepted January 5, 2016)

Abstract

This study employs the Lamb wave method to detect damage in Fiber–metal laminates (FMLs). The method is based on quasi-isotropic behavior approximation and beamforming techniques. Delay and sum and minimum variance distortionless response beamformers are applied to a uniform linear phased array. The simulation in finite element software is conducted to evaluate the performance of the presented procedure. The two types of damage studied are the following: (1) Delamination between fiber–epoxy and metal layers and (2) crack on the metal layer. The present study has the following important contributions: (1) Health monitoring of multi-damaged FMLs using Lamb waves and beamforming technique, (2) detection of damage type, (3) detection of damage size by 1D phased array, and (4) identification of damages that occurred very close to the laminate edges or close to each other.

Keywords: Beamforming; Damage detection; Fiber–metal laminates; Lamb wave

1. Introduction

In recent years, Fiber–metal laminates (FMLs) have been significantly developed in different industries, especially in the aerospace industry. FMLs have greater mechanical and chemical properties than isotropic materials. However, damage propagation in these structures leads to their sudden failure. FMLs, similar to other structures, are subject to various types of damage, such as delamination, corrosion and cracks. Damage identification in these structures is very important in preventing loss of life and property. Thus, this study focuses on Structural health monitoring (SHM) of FMLs.

This study has chosen the Lamb wave propagation method among the various SHM methods because of the following significant advantages: 1) Waves have the ability to propagate over a significant distance, 2) waves have high sensitivity to inhomogeneity and variation of geometry, 3) Lamb waves can be easily generated into structures using small pieces of piezoelectric ceramics, and 4) piezoceramic actuators/sensors can be permanently bonded to the surface of the structures to generate/receive Lamb waves [1, 2]. Lamb wave propagation using piezoceramics is more affordable than other SHM methods because of its permanent attachment and the low cost of piezoceramics.

Damage detection in plate-like structures is more complex than that in beam-like structures. Detection in plate-like structures requires several sensors and actuators instead of only one transducer as well as an advanced signal processing method. Some researchers have presented valuable information and techniques in this field. Rucka [3] studied wave propagation in a steel plate using a 2D spectral element based on Kane–Mindlin theory. Su et al. [4] discussed the interaction of wave with delamination in carbon/fiber epoxy laminate. They also used at least four piezoceramics localized on each corner of the laminate to identify one delamination. Rathod and Mahapatra [5] presented the triangulation method to localize corrosion in metallic plates by a circular array of piezoelectric wafers. They used at least three array elements to identify damage location using the time of flight of the reflected wave from damage. One of the disadvantages of the triangulation method is that the damage detection procedure becomes more complex, especially in composite structures, when the number of damages increases or when the reflected waves from the edges of the plate cannot be ignored. Therefore, researchers tend to use an array of piezoelectric elements to scan plate-like structures. Giurgiutiu and Bao [6] presented the embedded ultrasonic structural radar algorithm to detect damage in metallic plates using the pulse–echo configuration. They applied a Delay and sum (DAS) beamformer to a uniform linear array to scan the large plate area. Yu and Giurgiutiu [7] presented the required equations for near- and far-field beamforming.

*Corresponding author. Tel.: +98 17342723354

E-mail address: a_maghsoodi@aut.ac.ir

[†]Recommended by Associate Editor Kyeongseok Woo

© KSME & Springer 2016

They also compared circular and linear phased arrays in metallic plates. Ostachowicz et al. [8] proposed a star configuration of piezoelectric transducers containing four linear phased arrays for damage localization in an aluminum plate. Yan et al. [9] studied the influences of the anisotropy behavior of composite materials on the amplitude and velocity of Lamb waves. Engholm et al. [10, 11] applied the Minimum variance distortionless response (MVDR) beamformer to a 2D phased array on an aluminum plate. They compared the MVDR and DAS beamformers. The results showed that the former performs better than the latter in resolution and interfering mode suppressions.

Aside from the aforementioned research, several studies have also focused on FMLs as new applicable structures in different industries. Rosalie et al. [12] studied the variation of the Lamb wave group velocity in GLARE aluminum plates containing one delamination. They used two methods, namely, wedge ultrasonic probes and embedded piezoelectric in a glass fiber layer. Zukauskas and Kazys [13] examined the delamination parameters in a GLARE3-3/2 laminate using the air-coupled ultrasonic technique. Farias et al. [14] used ultrasonic probes to capture signals. They analyzed these signals in time and frequency domains to extract information on the location of damage that occurred in an FML. The literature shows that most of the researchers have studied metallic or fiber–glass composite structures. Moreover, most of them have investigated large plates and assumed damage locations far from the plate edges (i.e., approximately 20 cm) to avoid influences of reflected waves from the plate edges.

The present study aims to detect the location, size, and type of two different damages (i.e., delamination and crack) in a small multi-damaged FML in the presence of reflected waves from laminate edges using a uniform linear phased array. The two types of damage assumed in the FML are (1) delamination between fiber–epoxy and metal layers and (2) cracks on the metal layer. The change in the material properties of the fiber–epoxy layers of laminate in different directions leads to certain complexities in the damage detection procedure. The beamforming (phased array) and Quasi-isotropic behavior approximation (QIBA) techniques are used to overcome this problem. Some numerical examples are presented to clarify the proposed procedure. In these examples, healthy and damaged laminates are modeled in ABAQUS software. Two beamforming techniques (i.e., DAS and MVDR) are applied to a uniform linear array on the laminates. Their results are subsequently compared.

2. Formulation

This study conducts multi-damage detection in a small FML. This study faces the following two important challenges: (1) The displacement amplitude and the propagation velocity of the wave vary in different directions of wave propagation because of the anisotropic behavior of the fiber–epoxy layers of FML; and (2) compared to other papers, this

study considers a small FML to investigate the effects of the reflected waves from the laminate edges. These problems increase the complexities of the damage detection procedure in laminate. Therefore, two effective techniques are used, namely, the QIBA and beamforming methods. The necessary stages for damage identification using these techniques are presented in the sections that follow.

2.1 Quasi-isotropic behavior approximation of FML

This subsection presents an applicable strategy to overcome problem (1). The amplitude and velocity of the guided wave in composite structures vary in different directions because of the variation of material properties. Moreover, the direction of the energy propagation is not generally similar to that of the wave vector. The literature shows that the calculation of the angle difference between the directions of energy propagation and wave vector is complex. Therefore, this study extends the proposed method for FMLs in Refs. [9, 15] to eliminate the complicated calculation for angle difference as well as to reduce the significant variations of wave amplitude and phase velocity in different wave propagation directions. The standard deviation curve of the wave velocity in different wave propagation directions for various wave excitation frequencies is plotted through the QIBA technique. The effects of the anisotropic behavior diminish if the standard deviation approaches to zero. Consequently, each excitation frequency with the minimum amount of deviation is the best frequency because the wave velocity variation is less than that in other frequencies.

The equation for calculating the standard deviation σ is given as follows:

$$\sigma(\omega_j) = \sqrt{\frac{\sum_{i=1}^M (c_p(\theta_i, \omega_j) - \mu(\omega_j))^2}{M}}, \quad (1)$$

$$j = 1, 2, \dots, q$$

where θ , ω , and c_p are the wave propagation direction, excitation frequency, and phase velocity, respectively. M , q and μ are the number of wave propagation directions, number of excitation frequencies, and average of all phase velocities in different directions in the j th frequency, respectively.

2.2 Beamforming technique for FML

This subsection describes an effective method to solve problem (2). Piezoelectric sensors attached to the laminate receive signals through the pulse–echo method (Fig. 1). Received signals contain both reflected waves from laminate edges and damages. Therefore, distinguishing reflected waves caused by damages may be impossible from those caused by laminate edges. A powerful method is required to monitor the entire laminate area and to detect multiple damages. The

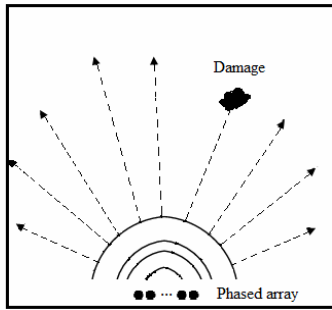


Fig. 1. Sending/receiving signals using the phased array attached to the damaged laminate.

beamforming technique is one of the most appropriate methods of amplifying desired reflected waves in a certain direction, θ , and attenuating undesired waves. A large area of the laminate can be inspected by changing θ over the laminate surface and applying a scanning beam. This study uses two different beamforming methods, including DAS and MVDR beamformers. Both methods are described in the sections that follow.

2.2.1 DAS beamformer

This study considers a uniform linear array with N identical elements, as shown in Fig. 2. In this figure, d and r are the spacing between the center of neighboring elements and between the center of the array and damage, respectively. Each element in the array is known as both actuator and sensor. All of the array elements individually receive the reflected signals when each element is excited as the actuator. This process is conducted through the pulse–echo method. The DAS beamforming method is based on applying an appropriate phase delay time on each array element to direct the array output in the specific direction. In this study, the phase delay time is relative to the center of the array. The resulting signal of the array, F , is the summation of the sensor outputs. The process is mathematically described as follows [9, 10]:

$$F(r, \theta) = \sum_{j=1}^N \sum_{i=1}^N w_j f_{ij} (t - \delta_{ij}(\theta)), \tag{2}$$

where delay time, δ_{ij} , is as follows:

$$\delta_{ij}(\theta) = -\frac{s_i \cos \theta}{c_p} - \frac{s_j \cos \theta}{c_p}, \tag{3}$$

where f_{ij} refers to the received signal by the j th element of the array as the sensor when the i th element is actuated. s_i , w_j , and s_j are the spacing between the center of the array and actuator i , amplitude weighting factor of sensor j , and the spacing between the center of the array and sensor j , respectively. Accordingly, $w_j = w_{DAS} = 1/N$ is used for the DAS method in this study. Eq. (2) may be rewritten in matrix

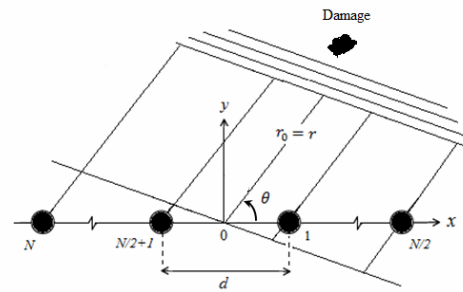


Fig. 2. Uniform linear phased array.

form as follows:

$$F(r, \theta) = W a^T(\theta) X(r, \theta) a(\theta), \tag{4}$$

where

$$X = \begin{bmatrix} f_{11} & f_{21} & \dots & f_{i1} & \dots & f_{N1} \\ f_{12} & f_{22} & & \vdots & & \vdots \\ \vdots & & \ddots & \vdots & & \vdots \\ f_{1j} & \dots & \dots & f_{ij} & \dots & \vdots \\ \vdots & & & \ddots & & \vdots \\ f_{1N} & \dots & \dots & \dots & \dots & f_{NN} \end{bmatrix}_{N \times N} \tag{5}$$

$$a^T(\theta) = [e^{-j\omega\delta_1(\theta)} \quad e^{-j\omega\delta_2(\theta)} \quad \dots \quad e^{-j\omega\delta_n(\theta)} \quad \dots \quad e^{-j\omega\delta_N(\theta)}] \tag{6}$$

$$\delta_n(\theta) = -\frac{s_n \cos \theta}{c_p}, \quad n = 1, 2, \dots, N. \tag{7}$$

$$W = [w_1 \quad w_2 \quad \dots \quad w_n \quad \dots \quad w_N]^T. \tag{8}$$

2.2.2 MVDR beamformer

One of the most common adaptive beamformers is the MVDR beamformer. The weight vector in this method is given by the following equation [10]:

$$W_{MVDR}(\theta) = \frac{\hat{R}^{-1} a(\theta)}{a^H(\theta) \hat{R}^{-1} a(\theta)}, \tag{9}$$

where the signal covariance matrix can be estimated as follows:

$$\hat{R} = \frac{1}{N_s} X X^H, \tag{10}$$

where N_s is the number of sampling points.

2.2.3 Calculation of damage location

As mentioned in the previous subsections, the beamforming methods result in a focused signal on a certain direction denoted by angle θ . Changing angle θ from 0 to 180 results in a virtual scanning beam over the laminate. Therefore, a large area of the laminate can be inspected. This procedure is

conducted for both intact and damaged laminates. Both resulting signals from the array in each angle θ are then compared. The damage in that direction is present if any additional wave packet in the damaged laminate in angle θ_0 is observed. The damage location in angle θ_0 relative to the center of the array, $r_{damage}(\theta_0)$, can be calculated as follows:

$$r_{damage}(\theta_0) = \frac{c_g(\theta_0)t_{damage}}{2}, \quad (11)$$

where $c_g(\theta_0)$ and t_{damage} are the group velocity and the flight time of the wave in angle θ_0 , respectively.

3. Numerical examples

All of the aforementioned procedures are used to detect the damages in the FML and illustrate and validate the presented methods. Consider a 30-by-30 cm² six-layer FML $[Al/0^\circ/90^\circ]_s$ with the following material and geometrical properties of a unidirectional glass fiber–epoxy layer:

material density, $\rho_c = 1540 \text{ kg/m}^3$,
 Young's modulus, $E_1 = 36, E_2 = E_3 = 5 \text{ MPa}$,
 shear modulus, $G_{12} = G_{13} = 2.7, G_{23} = 1.92 \text{ MPa}$,
 Poisson ratio, $\nu_{12} = \nu_{31} = 0.25, \nu_{32} = 0.301$,
 thickness, $h_c = 0.35 \text{ mm}$.

The following properties are considered for the Al layer:

thickness, $h_{Al} = 0.5 \text{ mm}$,
 material density, $\rho_{Al} = 2700 \text{ kg/m}^3$,
 Young's modulus, $E_{Al} = 72 \text{ MPa}$.

First, the range of the best excitation frequencies of the Lamb wave in healthy FML $[Al/0^\circ/90^\circ]_s$ is determined using the QIBA technique. Mode A_0 is chosen for damage detection because of two reasons. First, mode A_0 has a shorter wavelength, λ , than mode S_0 at a given excitation frequency. Therefore, damage detection is possible with smaller size. Second, the velocity of mode A_0 at low frequencies is less than that of mode S_0 , which is a great advantage in damage detection of small-size laminates because the reflected waves caused by the damages can be distinguished from those caused by the laminate edges.

The phase velocity of the wave in different directions and frequencies is calculated using the transfer matrix method presented in our previous paper [16]. The curve of the phase velocity standard deviations for mode A_0 for the wave launching directions from 0 to 180 with an angle increment of 20 has been calculated using Eq. (1) and is shown in Fig. 3. Second, an appropriate excitation frequency is selected to model a uniform linear phased array on the FML surface in ABAQUS software [17].

Fig. 3 shows that $f = 20 \text{ kHz}$ and $f = 160 \text{ kHz}$ have the maximum and minimum deviations, respectively. There-

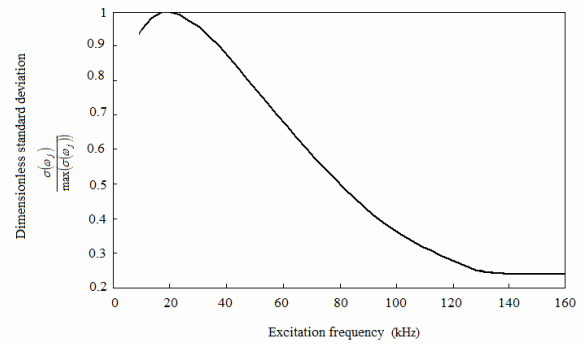


Fig. 3. Curvature of phase velocity standard deviations for mode A_0 .

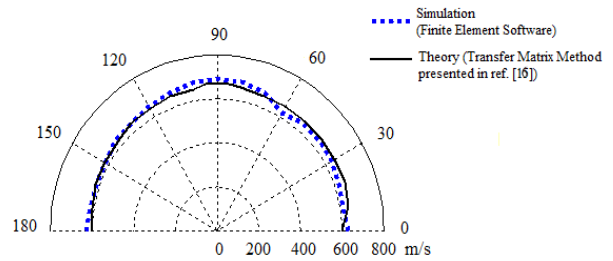


Fig. 4. Comparison of phase velocity of mode A_0 at $f = 100 \text{ kHz}$ calculated through theory and simulation.

fore, $f = 160 \text{ kHz}$ is appropriate for quasi-isotropic behavior approximation. The literature presents that the appropriate space between array elements is $d = \lambda / 2$. Accordingly, d at $f = 160 \text{ kHz}$ is too small and is not suitable to arrange the phased array. Therefore, a frequency that is lower than $f = 160 \text{ kHz}$ is selected to achieve suitable d . In this study, $f = 100 \text{ kHz}$ with the average phase velocity of $avg(c_p(\theta, 100)) = 641.8 \text{ m/s}$ and $\lambda = 6.418 \text{ mm}$ is selected to arrange the phased array equally spaced with $d = 3 \text{ mm}$ (Fig. 3). Note that at $f = 100 \text{ kHz}$, the wave has a quasi-isotropic behavior because it is close to $f = 160 \text{ kHz}$. The FML simulation is validated by obtaining the phase velocity profile of mode A_0 at $f = 100 \text{ kHz}$ using the transfer matrix method and simulation in ABAQUS software (Fig. 4). The phase velocity in various directions is approximately the same. Its profile also resembles a semicircle, such as isotropic plates (Fig. 4). In the simulations, a 12-element uniform linear phased array, which is equally spaced with $d = 3 \text{ mm}$, is considered. The radius of each element is 1 mm. The array is located at the edge of the laminate. Moreover, the anti-symmetric excitation method presented in Ref. [18] is used to generate mode A_0 . A five-cycle ton-burst windowed by Hanning is applied to the actuators as the excitation signal. Eq. (11) indicates that the group velocity of mode A_0 in different directions should be calculated. Therefore, the group velocity profile of mode A_0 has been obtained using the simulation (Fig. 5). The healthy laminate is considered as a base model to be compared with the damaged laminate for damage detection. Therefore, the DAS and MVDR beamformers are first applied

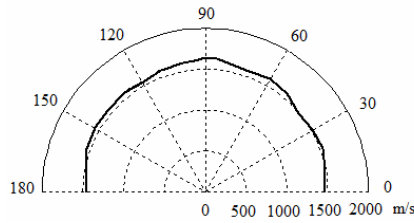


Fig. 5. Group velocity of mode A_0 at $f = 100$ kHz calculated through simulation.

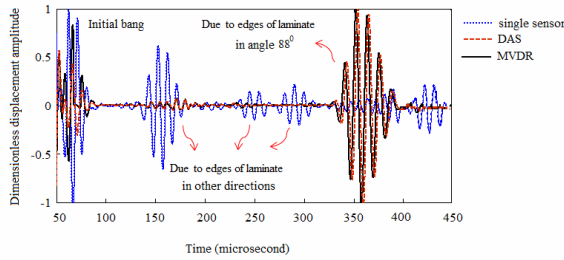


Fig. 6. Comparison of array output using DAS and MVDR beamformers with the output of the first sensor at $\theta = 88^\circ$ for the healthy FML $[Al/0^\circ/90^\circ]_s$.



Fig. 7. Modeling of delamination in ABAQUS software.

to the healthy FML $[Al/0^\circ/90^\circ]_s$. For example, the resulting signals of the array at $\theta = 88^\circ$ using the DAS and MVDR beamformers have been compared with the output of the first sensor in Fig. 6. This figure shows that both methods successfully eliminate the reflected waves from the laminate edges in other directions. A number of examples are presented in the following subsections to illustrate the damage detection procedure in the FML $[Al/0^\circ/90^\circ]_s$ using the beamforming methods.

3.1 Example 1: Laminate contains one delamination

A delamination at the center of the laminate between the fiber–epoxy and Al layers is examined in this example (Fig. 7). Two different cases are considered, including small and large delaminations, to study the effects of damage sizes on the output signals.

3.1.1 Laminate contains one large delamination

In this case, a square 2-by-2 cm^2 delamination is considered at the center of the laminate $[Al/0^\circ/90^\circ]_s$ between the first and second layers. Fig. 8 compares the resulting signals of the array at $\theta = 88^\circ$ with the output of the first sensor of the array. Two separate wave packets are observed at $t_1 = 168 \mu s$, $t_2 = 197 \mu s$, which are reflected waves from the front and rear edges of delamination, respectively. Consequently, calculating

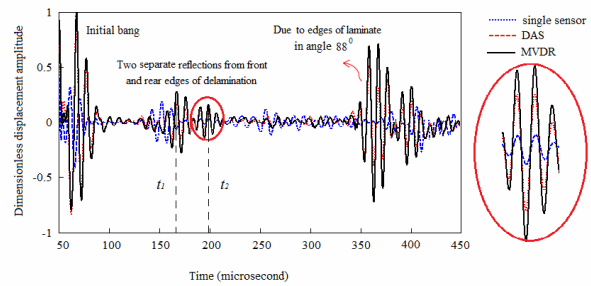


Fig. 8. Comparison of array output using DAS and MVDR beamformers with output of the first sensor at $\theta = 88^\circ$ for FML $[Al/0^\circ/90^\circ]_s$ containing a large delamination.

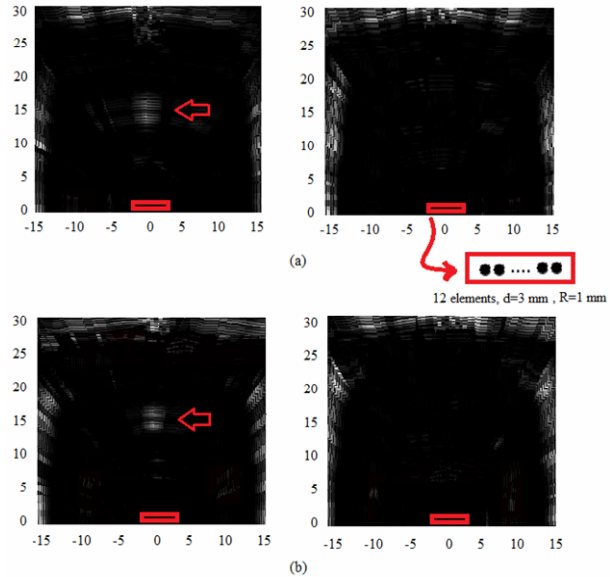


Fig. 9. Comparison of healthy (right) and damaged (left) FMLs $[Al/0^\circ/90^\circ]_s$ containing a large delamination using (a) DAS; (b) MVDR methods.

the delamination length using the time difference between two wave packets and Eq. (11) is possible. Fig. 5 shows that the group velocity of the wave is $c_g = 1640$ m/s. Therefore, the locations of the front and rear edges of delamination are obtained using Eq. (11): $x_1 = 13.77$ cm and $x_2 = 16.15$ cm. The actual locations are $x_1 = 14$ cm and $x_2 = 16$ cm. The minor errors are related to the use of the QIBA technique and a slight variation of the wave velocity in the delaminated structure.

The entire laminate area is scanned by applying the MVDR and DAS beamformers to the output signals of the sensors in different angles ranging from $\theta = 0^\circ$ to $\theta = 180^\circ$ with an angle increment of 5° . The results are shown in Fig. 9, where the right figures refer to the healthy laminate and the left ones refer to the damaged laminate. A comparison of the healthy and damaged laminates indicates a large delamination at the center of the laminate. The location, size, and number of damages can be detected by laminate scanning. Fig. 9 shows that both the DAS and MVDR beamformers can identify the delamination location and dimensions. However, the MVDR

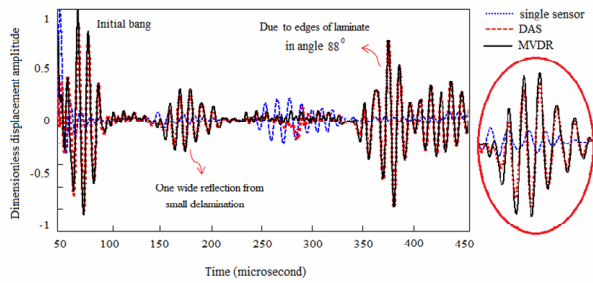


Fig. 10. Comparison of array output using DAS and MVDR beamformers with output of first sensor at $\theta = 88^\circ$ for FML $[Al/0^\circ/90^\circ]_s$ containing a small delamination.

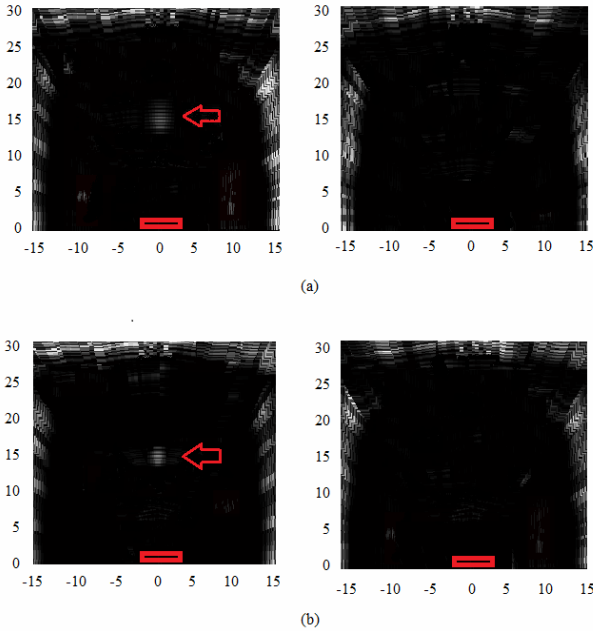


Fig. 11. Comparison of healthy (right) and damaged (left) FMLs $[Al/0^\circ/90^\circ]_s$ containing a small delamination using (a) DAS; (b) MVDR methods.

method more accurately reinforces the desired signals and eliminates the undesired ones.

3.1.2 Laminate contains a small delamination

In this example, the laminate contains a square 1-by-1 cm² delamination at the same location as that of the previous example. The procedure mentioned in the previous example is repeated. Fig. 10 compares the resulting signals of the array at $\theta = 88^\circ$ with the output of the first sensor of the array. This figure shows only one fairly wide wave packet instead of two separate wave packets such as those in the previous example. The reason is that the delamination is small. Therefore, two reflected waves from the front and rear edges of the delamination are integrated. Fig. 11 compares the scans of the healthy and damaged laminates obtained using the DAS and MVDR beamformers. A single, wide wave packet in Fig. 11 indicates a small delamination in the damaged laminate.

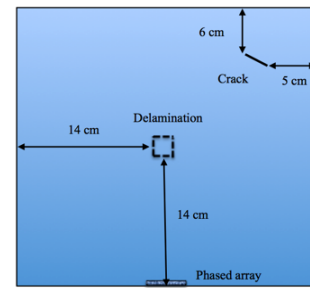


Fig. 12. Model of delamination and inclined crack.

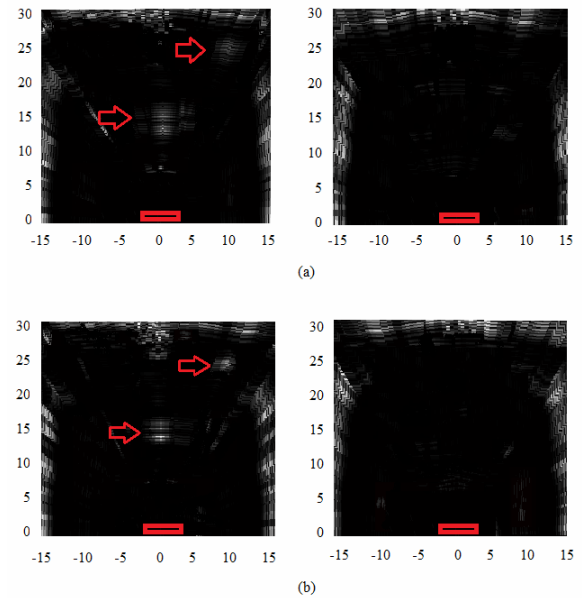


Fig. 13. Comparison of healthy (right) and damaged (left) FMLs $[Al/0^\circ/90^\circ]_s$ containing a large delamination and an inclined crack using (a) DAS; (b) MVDR methods.

3.2 Example 2: Laminate contains a delamination and an inclined crack

The two different damages in the FML modeled in this example are as follows: (1) a square 2-by-2 cm² delamination at the same location as example (1) and (2) an inclined 2.2 cm crack with 0.25 mm depth on the first layer of the laminate $[Al/0^\circ/90^\circ]_s$. The crack is modeled as a notch close to the laminate edges (Fig. 12). This example mainly aims to study the effects of the reflected waves from the laminate edges as well as the number, type, and angular position of the damages. The DAS and MVDR beamformers are applied to the output signals of the sensors. Fig. 13 compares the scans of healthy and damaged laminates. This figure indicates that both beamformers have acceptable results and can detect both damages in the laminate. However, the MVDR beamformer is more successful than the DAS beamformer in eliminating the interference waves and reinforcing the main beam.

Moreover, each damage type is detected using the type of reflected wave packets (i.e., two separate reflected wave pack-

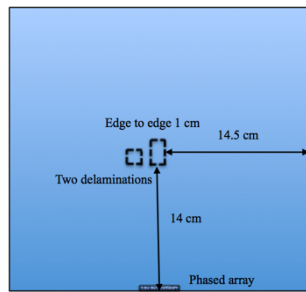


Fig. 14. Model of two near delaminations.

ets and one narrow wave packet refer to a large delamination and crack, respectively). In previous research, damage locations are usually assumed to be far from the laminate edges, that is about 20 cm, to avoid the influences of the reflected waves that these edges cause. In this example, the smallest distance between the crack and the laminate edges is 5 cm. The proposed method can successfully detect damages even those very close to the laminate edges (Fig. 13). An important factor for these results is the selection of the appropriate excitation frequency and Lamb mode. When damage is close to the laminate edges, if we select a low-velocity wave, the reflected waves from the edges and damages are less integrated with each other. Therefore, distinguishing these reflected waves is easy. This example shows that detecting the damage types even near the edges is possible by choosing the appropriate Lamb wave mode and excitation frequency.

3.3 Example 3: Laminate contains two near delaminations

Fig. 14 shows two modeled delaminations that are close to each other in the FML (i.e., a rectangular 1-by-2 cm² delamination and a square 1-by-1 cm² delamination). The distance between the two damages is 1 cm. This example mainly aims to study the effect of damage closeness on signals. The DAS and MVDR beamformers are applied to the output signals of the sensors. The presented procedure can detect two damages that are very close to each other (Fig. 15). The damaged area is detectable, whereas the boundary between the damages is not very clear. The two separate reflected wave packets in Fig. 15 refer to the presence of a large delamination, while the wide reflected wave packet refers to a smaller delamination.

4. Conclusions

This paper presents an applicable procedure to monitor the health of FMLs using the Lamb wave propagation method. The study mainly aims to (1) decrease the variation of amplitude and velocity of Lamb waves in the FMLs using the QIBA technique; (2) detect the number, type, location, and size of damages that occur in the FMLs; (3) study the effects of two close damages on the output signals; and (4) diminish the effect of reflected waves from the laminate edges to detect the

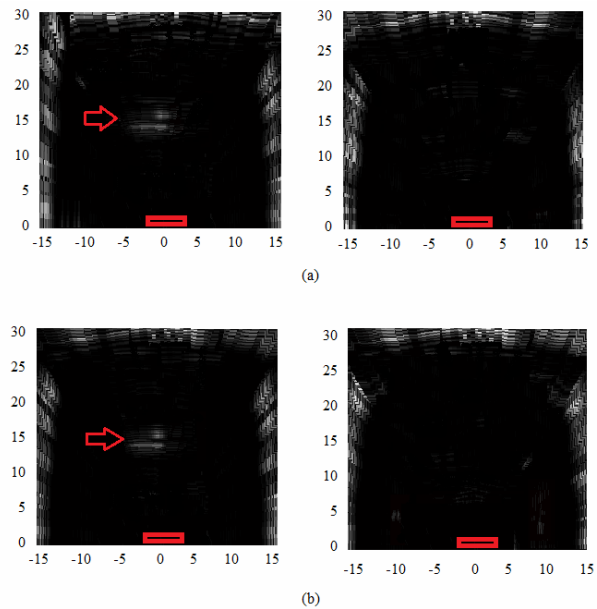


Fig. 15. Comparison of healthy (right) and damaged (left) FMLs $[Al/0^\circ/90^\circ]$, containing two near delaminations using (a) DAS; (b) MVDR methods.

damages close to the edges. The beamforming and QIBA techniques are applied to a uniform linear phased array. The presented procedure is illustrated and validated by modeling two types of damages in a small FML $[Al/0^\circ/90^\circ]$, including small and large delaminations between the glass fiber-epoxy and metal layers and the crack on the metal layer that is very close to the laminate edges. One of the most important factors in damage detection in composite materials is the selection of appropriate excitation frequency and Lamb mode. Mode A_0 with the best excitation frequency is found using the QIBA technique. Two common beamformers (i.e., DAS and MVDR) are used. Their results are then subsequently compared. The present study provides the following contributions, which have not been clearly mentioned in previous papers: (1) Detection of multiple damages in small FMLs using Lamb waves and the beamforming technique; (2) identification of the damage type using the reflected waves from damages (i.e., two separate reflected wave packets and one wide wave packet refer to a large delamination and a small delamination, respectively, and one narrow wave packet refers to the presence of a crack); (3) detection of damage sizes (width and length) by a linear phased array; and (4) detection of the damages that occurred very close to the laminate edges or very close to each other.

References

- [1] Z. Su and L. Ye, *Identification of damage using Lamb waves: from fundamentals to applications*, Springer (2009).
- [2] A. Ghadami, M. Behzad and H. R. Mirdamadi, A mode conversion-based algorithm for detecting rectangular notch

- parameters in plates using Lamb waves, *Archive of Applied Mechanics*, 85 (6) (2015) 793-804.
- [3] M. Rucka, Modelling of in-plane wave propagation in a plate using spectral element method and Kane–Mindlin theory with application to damage detection, *Archive of Applied Mechanics*, 81 (12) (2011) 1877-1888.
- [4] Z. Su, L. Ye and X. Bu, A damage identification technique for CF/EP composite laminates using distributed piezoelectric transducers, *Composite Structures*, 57 (1-4) (2002) 465-471.
- [5] V. T. Rathod and D. M. Roy, Ultrasonic Lamb wave based monitoring of corrosion type of damage in plate using a circular array of piezoelectric transducers, *NDT & E International*, 44 (7) (2011) 628-636.
- [6] V. Giurgiutiu and J. Bao, Embedded-ultrasonics structural radar for in situ structural health monitoring of thin-wall structures, *Structural Health Monitoring*, 3 (2) (2004) 121-140.
- [7] L. Yu, V. Giurgiutiu, In-situ optimized PWAS phased arrays for Lamb wave structural health monitoring, *Journal of Mechanics of Materials and Structures*, 2 (3) (2007) 459-487.
- [8] W. Ostachowicz, T. Wandowski and P. Malinowski, Elastic wave phased array for damage localisation, *Journal of Theoretical and Applied Mechanics*, 46 (4) (2008) 917-931.
- [9] F. Yan, *Ultrasonic guided wave phased array for isotropic and anisotropic plates*, Pennsylvania: Pennsylvania State University (2008).
- [10] M. Engholm, T. Stepinski and T. Olofsson, Imaging and suppression of Lamb modes using adaptive beamforming, *Smart Materials and Structures*, 20 (8) (2011) 085024.
- [11] M. Engholm and T. Stepinski, Adaptive beamforming for array imaging of plate structures using Lamb waves, *IEEE Transactions on Ultrasonics, Ferroelectrics and Frequency Control*, 57 (12) (2010) 2712-2724.
- [12] R. C. Rosalie, M. Vaughan, A. Bremner and W. K. Chiu, Variation in the group velocity of Lamb waves as a tool for the detection of delamination in GLARE aluminium plate-like structures, *Composite Structures*, 66 (1) (2004) 77-86.
- [13] E. Žukauskas and R. Kažys, Investigation of the delamination type defects parameters in multilayered GLARE3-3/2 composite material using air-coupled ultrasonics technique, *Ultrasonics (Ultrasound)*, 62 (2007) 44-48.
- [14] C. T. Farias, E. F. Filho, Y. T. Santos and I. S. Araujo, Spectral analysis of the propagation of Lamb waves on fibre-metal laminated plates to detect and evaluate different defects, *Proc. of 18th World Conference on Nondestructive Testing*, Durban, South Africa (2012).
- [15] F. Yan and J. L. Rose, Guided wave phased array beam steering in composite plates, *Proceedings of SPIE, Health Monitoring of Structural and Biological Systems* (2007) 6532-65320G.
- [16] A. Maghsoodi, A. R. Ohadi and M. Sedighi, Calculation of wave dispersion curves in multilayered composite-metal plates, *Shock and Vibration* (2014) ID:410514.
- [17] *Dassault System: ABAQUS 6.10: Analysis user's manual*, Dassault Systèmes Simulia Corp., Providence RI (2010).
- [18] Z. Su and L. Ye, Selective generation of Lamb wave modes and their propagation characteristics in defective composite laminates, *Journal of Materials Design and Applications*, 218 (2) (2004) 95-110.



Ameneh Maghsoodi is a Ph.D. student of mechanical engineering, University of Michigan, Michigan, US. She received her Master degree in mechanical engineering from Amirkabir University of Technology. Her research interests include structural health monitoring, composite materials, bio-nano technology, dynamics and vibration.